Role of Electrostatic Interactions in SH2 Domain Recognition: Salt-Dependence of Tyrosyl-Phosphorylated Peptide Binding to the Tandem SH2 Domain of the Syk Kinase and the Single SH2 Domain of the Src Kinase†

Richard A. Grucza, J. Michael Bradshaw, Vesselin Mitaxov, and Gabriel Waksman*

Department of Biochemistry and Molecular Biophysics, Washington University School of Medicine, 660 South Euclid Avenue, Saint Louis, Missouri 63110, USA

Received April 19, 2000; Revised Manuscript Received June 23, 2000

ABSTRACT: SH2 domains are small protein domains that bind specifically to tyrosyl-phosphorylated sequences. Because phosphorylation contributes a large part of the binding free energy, it has been postulated that electrostatic interactions may play an important role in SH2 domain recognition. To test this hypothesis, we have examined the salt dependence of the interaction between tyrosyl-phosphorylated peptides and SH2 domains. The dependence of the binding constant, K_{obs}, on [NaCl] was shown to be strong for binding of the tandem SH2 domain of the Syk kinase (Syk-tSH2) to doubly phosphorylated peptides derived from immune-receptor tyrosine activation motifs (dpITAMs): the slopes of plots of log(K_{obs}) versus log [NaCl], designated SK_{obs}, ranged from -2.6 ± 0.1 to -3.1 ± 0.2. Binding of the single SH2 domain of the Src kinase to its consensus singly phosphorylated peptide (sequence pYEEI where pY indicates a phosphotyrosine) was also highly dependent on [NaCl] with a SK_{obs} value of -2.4 ± 0.1. The ability of salt to disrupt the interactions between Syk-tSH2 and dpITAM peptides was shown to be anion-dependent with the inhibitory effect following the order: phosphate > Cl^- > F^-. For the Syk-tSH2 system, interactions in the pY-binding pockets were shown to be responsible for a large portion of the total salt dependence: removal of either phosphate from the dpITAM peptide reduced the magnitude of SK_{obs} by 40−60% and weakened binding by 2−3 orders of magnitude. Consistent with this finding, binding of the single amino acid Ac-pY-NH_2 was characterized by a large salt dependence of binding and was also dependent on the identity of the perturbing anion. The role of peptide residues C-terminal to the pY, which are implicated in determining the specificity of the phosphopeptide−SH2 domain interaction, was next probed by comparing the binding of the Src SH2 domain to a peptide containing the pYEEI sequence with that of a lower affinity variant pYAAI peptide: the magnitude of SK_{obs} for the variant peptide was reduced to -1.3 ± 0.1 as compared to -2.4 ± 0.1 for the pYEEI peptide, indicating that in addition to pY, residues conferring peptide binding specificity contribute significantly to the salt dependence of SH2 domain binding. This study shows that electrostatic interactions play important roles not only in mediating pY recognition and binding but also in contributing to the specificity of the interactions between tyrosyl phosphopeptides and SH2 domains.

Src homology 2 (SH2)[1] domains are protein domains of ∼100 amino acids that have evolved to recognize and bind specifically to tyrosyl-phosphorylated sequences located on proteins involved in signal transduction (*1*, *2*). Their role is to facilitate recruitment of signaling proteins to tyrosine-phosphorylated sites, thereby promoting protein−protein interactions essential to propagation of cellular signals to various parts of the cell. SH2 domains all have a simple architecture consisting of a central β-sheet flanked by two α-helices (Figure 1A) (*3*). The β-sheet divides the structure into two parts. On one side, residues form a deep positively charged pocket into which the phosphotyrosine (pY) of the target inserts. On the other side of the β-sheet, a binding interface is formed that interacts specifically with the residues C-terminal to the pY. Residues in the SH2 domain that participate in this interface are not well-conserved among SH2 domains and, for this reason, are presumed to be responsible for determining peptide binding specificity.

Recently, the role in binding of each residue in an entire SH2 domain−tyrosyl phosphopeptide interface, that of the SH2 domain of the Src kinase and its consensus high affinity peptide (sequence pYEEI), has been investigated (*4*−*8*). These studies have shown that interactions in the pY-binding pocket contribute substantially more to binding than interactions at the rest of the interface. Additional studies aimed at investigating the role of the ionization state of the pY in binding have shown that reducing the charge of the phosphate results in greatly reduced binding affinity (*9*). Altogether,

† This work was funded by NIH Grant GM60231.

* To whom correspondence should be addressed at Department of Biochemistry and Molecular Biophysics, Washington University School of Medicine, 660 South Euclid Ave., Campus Box 8231, Saint Louis, MO 63110. Tel: (314) 362-4562. Fax: (314) 362-7183. Email: waksman@biochem.wustl.edu.

[1] Abbreviations: SH2, Src homology 2; Syk-SH2, tandem SH2 domain of Syk kinase; ITAM, immune-receptor tyrosine activation motif; mpITAM, monophosphorylated ITAM; dpITAM, doubly phosphorylated ITAM; pY, phosphotyrosine.

10.1021/bi000891n CCC: $19.00
Published on Web 07/28/2000

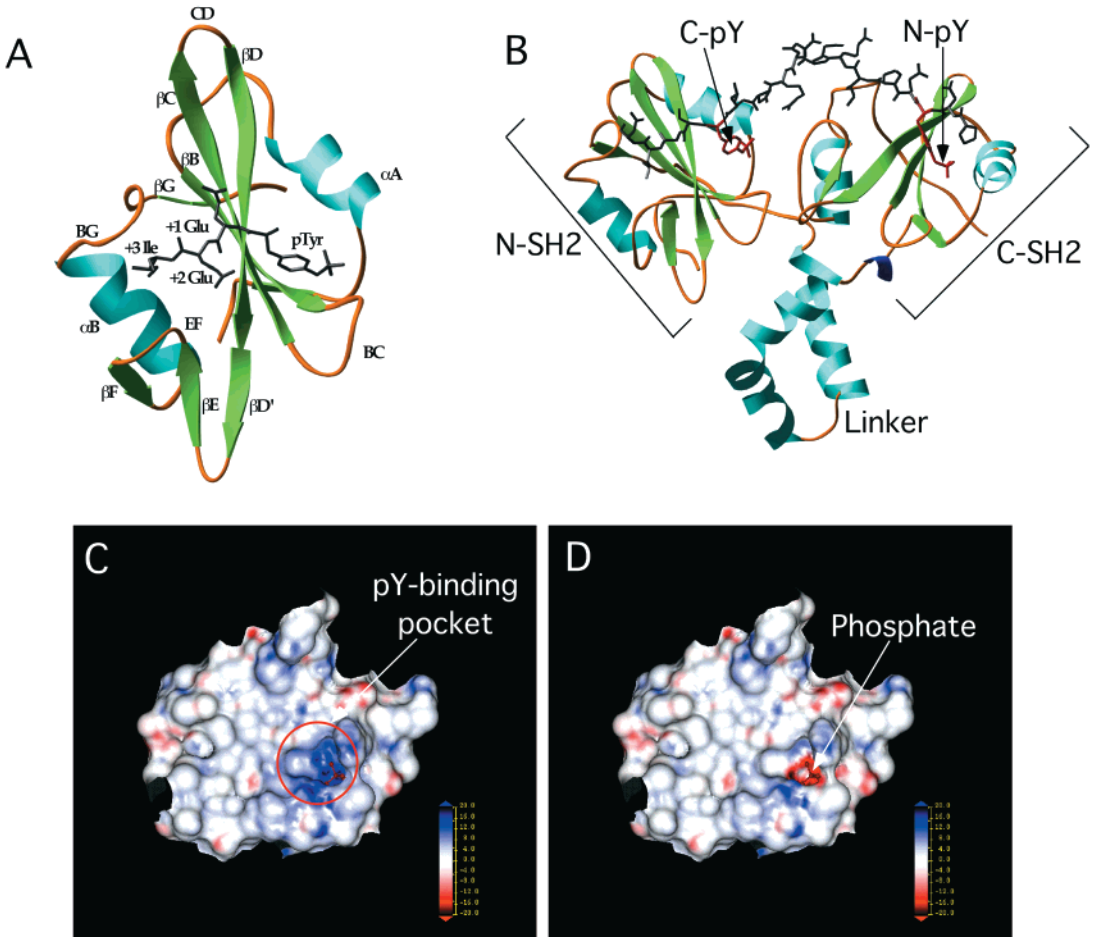

FIGURE 1: (A) Ribbon diagram of the Src SH2 domain−pYEEI peptide complex structure (*5*). Helices and *β*-strands are in cyan and green, respectively. The pYEEI peptide is in stick representation. Notation for secondary structures are as in ref *5*. (B) Ribbon diagram of the Syk-tSH2−CD3-*ϵ* dpITAM peptide complex (*18*). The N-terminal SH2 domain (labeled N-SH2), C-terminal SH2 domain (labeled C-SH2), and inter-SH2 linker (labeled linker) are shown. The CD3-*ϵ* dpITAM peptide is in stick representation with the atoms in the pYs in red. The C- and N-terminal pYs are labeled. (C) Surface electrostatic potential at the Src SH2 domain binding interface. The surface potential is calculated using the program DELPHI (*30*) and displayed using InsightII 95.0 (Biosym/MSI, San Diego). The red circle locates the pY-binding pocket. A phosphate group is shown bound to the pocket. This group, shown in ball-and-stick representation color-coded in red, is from the apo form of the Src SH2 domain structure (*4*). In this figure, the phosphate group was not included in the calculation of the electrostatic potential. (D) As in panel C except that, in this figure, the phosphate group was included in the calculation of the electrostatic potential. In panels C and D, the scales (in kcal/mol-*e*) for the potentials are shown in the lower right corner.

these studies have suggested that recognition of tyrosyl phosphopeptides by SH2 domains is likely to have a strong electrostatic component.

To test this hypothesis, we have examined the salt dependence of binding of tyrosyl phosphopeptides to the SH2 domains of two protein tyrosine kinases, the SH2 domain of the Src kinase (Src SH2 domain) and the "tandem SH2 domain" of the Syk kinase (Syk-tSH2). While the Src kinase contains only one SH2 domain, the Syk kinase contains two SH2 domains located in tandem. The tandem SH2 domain facilitates recruitment of Syk to tyrosine-phosphorylated sites, known as immune-receptor tyrosine activation motifs, or ITAMs, which have the consensus sequence YXX(L/I)-$X_{7/8}$-YXX(L/I) (*10*, *11*); receptor activation leads to phosphorylation of the two tyrosines of the ITAM, thereby creating a high affinity binding site for the tandem SH2 domain of Syk (see Figure 1B for details).

A thermodynamic signature of processes with a large electrostatic component is a strong dependence of the binding constants on solution salt concentration. Such an effect results in part from the ability of ions to "screen" electrostatic interactions, i.e., to nonselectively attenuate electrostatic potentials by increasing the effective dielectric constant of the solvent as predicted by the Debye−Hückel theory. Attempts have been made to partition the binding free energy into electrostatic and nonelectrostatic components on the basis of the salt dependence of binding using a Debye−Hückel theoretical framework. Such an approach was used, for example, to study the role of electrostatic interactions in the binding of thrombin to hirudin (*12*). It was later shown, however, that for the thrombin−hirudin system, the type of salt used to adjust ionic strength had a significant effect on the free energy of binding, a result that cannot be explained by a simple screening mechanism of salt (*13*). The frequency with which free energies of biomolecular interactions depend on the identity of the salt, and not simply ionic strength, underscores the need to understand the mechanism of salt-dependent free energy perturbation on a case-by-case basis (e.g., refs *14*−*17*).

In the study presented here, we investigate the ability of various salts to alter the binding free energy of several dpITAM peptides to Syk-tSH2. We show that binding is

strongly dependent on salt concentration and the magnitude of the salt effect is dependent on anion type. A large portion of the effect is caused by disruption of electrostatic interactions at the pY-binding pocket, confirming the predominant role of this region of the SH2 domains in molecular recognition of tyrosyl-phosphopeptides. However, these interactions do not account for the totality of the salt effect, an observation that leads us to examine the role of peptide residues C-terminal to the pY that are known to determine the specificity of the tyrosyl phosphopeptide−SH2 domain interaction. The results suggest that favorable electrostatic interactions between tyrosyl phosphopeptide targets and SH2 domain residues may be an important component of high affinity binding.

MATERIALS AND METHODS

Protein Expression and Purification. Syk tandem-SH2 domain and the Src SH2 domain were expressed and purified as described previously (*18*−*20*). Purity was assessed by SDS−PAGE and determined to be >95%. Prior to all experiments, exhaustive dialysis was carried out into a standard experimental buffer consisting of 50 mM HEPES, 150 mM NaCl, 1 mM EDTA, and 5 mM β-mercaptoethanol at pH 7.5. Salt concentration was adjusted after dialysis with either high salt or salt-free buffer. Protein concentrations were determined using the previously reported extinction coefficients (*19*, *20*).

Tyrosine Phosphopeptides. Tyrosine-phosphorylated peptides and acetylated, amidated phosphotyrosine (Ac-pY-NH_2) were obtained from Quality Controlled Biochemicals (Hopkinton, MA). Peptide concentrations were determined using an extinction coefficient of 1304 M^{-1} cm^{-1} at 267 nm for the doubly phosphorylated ITAM (dpITAM) peptides and 2079 M^{-1} cm^{-1} at 267 nm for monophosphorylated ITAM (mpITAM) peptides. The extension coefficient for the single phosphotyrosine ligands of the Src SH2 domain is 652 M^{-1} cm^{-1}. These numbers are based on an extinction coefficient for phosphotyrosine of 652 M^{-1} cm^{-1} (*21*) and represent the sums of extinction coefficients for tyrosine (*22*) and/or phosphotyrosine. Peptides were dissolved directly into the experimental buffer. When Ac-pY-NH_2 was used, it was dissolved into the experimental buffer, and the pH was adjusted to pH 7.5. Dialysis was then carried out in 200-Da molecular weight cutoff dialysis tubing to remove excess salt.

Fluorescence Titrations. Fluorescence titrations were carried out to determine the binding constants for dpITAM peptides by monitoring intrinsic tryptophan fluorescence of Syk-tSH2 as described in ref *19*. In brief, the titrations were carried out on an SLM 8000 spectrofluorimeter equipped with a water-jacketed cell turret that was used to control temperature. An excitation wavelength of 295 nm was used, a wavelength at which phosphotyrosine has negligible absorbance. In quartz cuvettes, 1.8−2.0 mL solutions of 200−250 nM Syk-tSH2 were titrated by incremental addition of peptide solutions at concentrations of 40−600 μM, depending on the anticipated binding constant. Solutions were incubated for 3 min or more prior to reading the fluorescence intensity. Emission wavelength was selected using a monochromator centered at 345 nm, the wavelength at which the intensity difference between the ligated and the unligated forms of Syk-tSH2 is maximal. Slit widths were 2 mm for excitation and 16 mm for emission. All experiments were conducted at 20 °C. Minor corrections for loss of signal due to photobleaching were applied to the intensity measurements. Plots of normalized fluorescence intensity versus total ligand concentration were prepared for each titration. Data were fit to a single-site binding model to determine the binding constant, K_{obs}, and the fluorescence at the end point of the titration (F_∞). In instances in which two or more titrations were conducted for a given set of conditions, all data were fit to a single value for K_{obs}.

For the monophosphorylated peptides, which bound with lower affinity and induced a weaker fluorescence change in the protein, binding constants at higher salt concentrations were determined by competitive titration. For these experiments, titrations were conducted using the CD3-ϵ dpITAM peptide as titrant at several fixed concentrations of the mpITAM peptide as competitor. All data for a given salt concentration were simultaneously fit to a model that determined the binding constant for the CD3-ϵ dpITAM peptide, the binding constant for the competitor, and the F_∞ for each individual titration.

Isothermal Titration Calorimetry for the Src-SH2 Domain. Binding of the pYEEI and pYAAI phosphopeptides to the Src SH2 domain was characterized by isothermal titration calorimetry using the protocols and conditions previously described (*6*). Experiments were conducted at 20 °C, pH 7.5, in 20 mM HEPES, 1 mM EDTA, and 1 mM β-mercaptoethanol, and various concentrations of NaCl.

Data Analysis. All nonlinear least-squares fitting was performed with the program Scientist (Micromath, Salt Lake City, UT). Reported uncertainties for nonlinear fits to determine binding constants represent 65% confidence limits computed in Scientist using the support plane method. Uncertainties associated with the slopes of log K_{obs} versus log [salt] plots (defined in the text as SK_{obs} when NaCl only is used or SK'_{obs} when other salts in addition to 150 mM NaCl are used) were determined by standard linear regression techniques; 65% confidence limits are reported.

RESULTS

Dependence of dpITAM Binding to Syk-tSH2 on NaCl Concentration. The sequences and naming conventions for the peptides used in this study are shown in Table 1. Three dpITAM peptides were examined: (i) a peptide derived from the CD3-ϵ chain of the T cell receptor (referred to as CD3-ϵ); (ii) a peptide derived from the γ-chain of the FcϵRI receptor, which is an Fc receptor to IgE (referred to as FcR-γ); and (iii) a peptide derived from the single chain Fc receptor class IIA, which is an Fc receptor to IgG (referred to as FcR-II). Binding constants were determined by monitoring intrinsic tryptophan fluorescence of Syk-tSH2 as a function of peptide concentration at 20 °C (*19*). Representative titrations for the CD3-ϵ dpITAM peptide at various salt concentrations are shown in Figure 2A. Titrations for each of the dpITAM peptides listed in Table 1 at 350 mM NaCl are shown in Figure 2B. Note that the overall quenching was dramatically reduced for binding of the FcR-II peptide relative to the other dpITAM peptides. As shown in Table 1, this ITAM is longer than the canonical ITAM sequence. We speculate that the reduced quenching is related to the ability of the two SH2 domains to adopt a different

Table 1: Sequences of Peptides Used in This Study[a]

	ITAMs																							
CD3-ϵ	P	**D**	Y*	**E**	P	I	*R*	*K*	G	-	-	-	-	-	Q	*R*	**D**	L	**Y***	S	G	L	N	Q	*R*
FcR-γ	G	V	**Y***	T	G	L	S	T	*R*	-	-	-	-	-	N	Q	**E**	T	**Y***	**E**	T	L	*K*	H	**E**
NC*	G	V	Y	T	G	L	S	T	*R*	-	-	-	-	-	N	Q	**E**	T	**Y***	**E**	T	L	*K*	H	**E**
N*C	G	V	**Y***	T	G	L	S	T	*R*	-	-	-	-	-	N	Q	**E**	T	Y	**E**	T	L	*K*	H	**E**
FcR-II	G	G	**Y***	M	T	L	N	P	*R*	A	P	T	**D**	**D**	**D**	*K*	N	I	**Y***	L	T	L	P	P	N

	Src SH2 domain ligands													
pYEEI	P		Q		**Y***		**E**		**E**		I		P		I
pYAAI	P		Q		**Y***		A		A		I		P		I

[a] Peptides were acetylated at the N-terminus and amidated at the C-terminus. Negatively charged residues are listed in boldface type, positively charged residues are indicated by italics. Y* indicates phosphotyrosine.

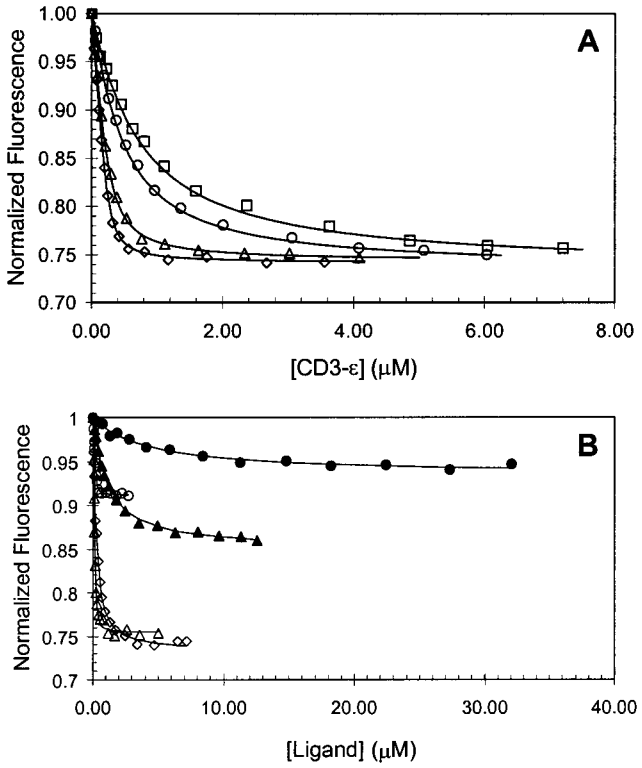

FIGURE 2: Representative fluorescence titrations of Syk-tSH2: (A) With the CD3-ϵ dpITAM peptide at various NaCl concentrations: 150 (open diamond), 250 (open triangle), 450 (open circle), and 600 mM (open square) NaCl. (B) With various ligands: CD3-ϵ (open diamonds), FcR-γ (open triangles), and FcR-II (open circles), dpITAM peptides at 350 mM NaCl and the mpITAMs NC* (filled triangles) and N*C (filled circles) at 150 mM NaCl. The fluorescence signal normalized to protein concentration and initial fluorescence is shown as a function of total ligand concentration at a constant protein concentration of 250 nM. Solid lines represent fits to a single-site binding model with resulting K_{obs} values plotted in Figure 3A.

relative orientation to accommodate the longer sequence, as discussed in refs *18* and *19*.

Binding of the CD3-ϵ dpITAM peptide was investigated at salt concentrations ranging from 50 to 1000 mM NaCl. For the FcR-γ and FcR-II dpITAM peptides, binding was too tight to measure accurately at salt concentrations below 250 mM using direct titration. However, we were able to estimate the binding constants for these peptides at 150 mM NaCl by using the competitive inhibitor Ac-pY-NH_2 (acetylated and amidated pY residue) at concentrations of 20−25 mM to perturb binding. Binding constants in the absence of inhibitor were then determined by using eq 4 (see details below), which describes K_{obs} as a function of [Ac-pY-NH_2] and K_{comp}, the apparent binding constant of the competitor (see below and Figure 5 for determination of K_{comp}). As a control, binding constants for the FcR-γ dpITAM peptide at 250 mM NaCl were determined both by direct titration and by the pY perturbation method and were identical within error (data not shown).

Results for the salt dependence of the association constants, K_{obs}, for all three dpITAM peptides examined are shown in Figure 3A. The slope of the log(K_{obs}) versus log [NaCl] plots (defined as SK_{obs}) is approximately constant above 150 mM NaCl, and the reported values of SK_{obs} reflect slopes taken over this range; these values are listed in Table 2. The values of SK_{obs} range from -2.6 ± 0.1 for the CD3-ϵ dpITAM peptide to -3.1 ± 0.2 for the FcR-γ dpITAM peptide. Hence an increase of 1 order of magnitude in [NaCl] concentration results in a 2−3 order of magnitude decrease in binding affinity. These results suggest a significant contribution of electrostatic interactions to binding (see Discussion).

Anion Dependent Effect. To establish whether NaCl acts exclusively via a nonspecific screening effect or perturbs binding in a salt-specific manner, we investigated the ability of NaF to disrupt binding. We focused on possible effects of anions because of the highly basic nature of the pY-binding pockets (Figure 1C). The fluoride anion has a high energy of hydration and is expected to be the least effective of the monovalent anions at penetrating the surface of a protein (*23*, *24*). Therefore, if interaction with the protein surface is part of the mechanism by which the anion attenuates binding, F^- should perturb binding less effectively than Cl^-. Binding constants for the CD3-ϵ dpITAM peptide were measured in the presence of 150 mM NaCl with NaF concentrations ranging from 0 to 600 mM (NaCl was included in the solution because Cl^- was required for protein solubility). As shown in Figure 3B, the slope of a log−log plot of K_{obs} versus total salt concentration ([NaCl] + [NaF]), defined as SK'_{obs},[2] shows that F^- is markedly less effective than Cl^- at disrupting binding of the CD3-ϵ dpITAM peptide to Syk-tSH2 (SK'_{obs} value of -1.0 ± 0.1). Binding constants for the FcR-γ dpITAM peptide were also measured as a function of [NaF] but were too high to measure accurately except at the highest NaF concentrations, 450 and 600 mM (Figure 4B). However, an estimate of SK'_{obs} was obtained using these two points and the value of K_{obs} at 150 mM NaCl in the absence of NaF derived from the pY perturbation experiments described above. This yielded a value of SK'_{obs} of -1.6, which is significantly less negative than the SK_{obs}

[2] See also Materials and Methods for usage of the "prime" superscript on SK_{obs}.

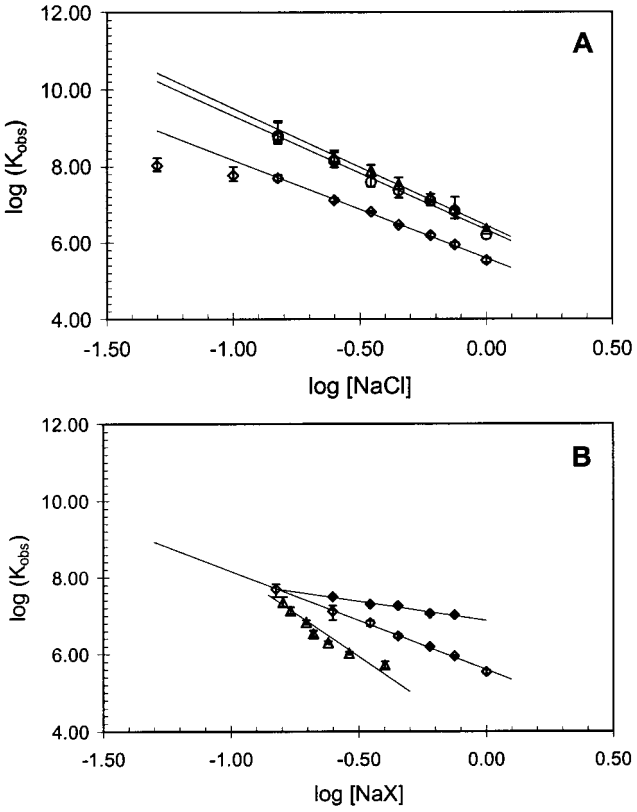

FIGURE 3: Salt dependence of the binding of dpITAM peptides to Syk-tSH2. (A) Logarithm of binding constants, K_{obs}, for the CD3-ϵ (open diamond), FcR-γ (open triangle), and FcRII (open circle) dpITAM peptides as a function of log [NaCl]. Error bars represent 95% confidence limits. (B) Comparison of the effects of fluoride, chloride, and phosphate. Logarithm of K_{obs} for the CD3-ϵ dpITAM peptide as a function of the logarithm of total salt concentrations ([NaCl], ([NaF] + [NaCl]), or ([Na_2-HPO_3] + [NaH_2PO_3] + [NaCl]) for NaCl only (open diamond), NaF added to 150 mM NaCl (filled diamond), and sodium phosphate added to 150 mM NaCl (open triangles). Each point represents 2−4 individual titrations, simultaneously fit to determine the binding constant. Error bars for the NaF data are not shown but are approximately the same size as the symbol height. Straight lines are least-squares fits to data at 150 mM salt concentration and higher. Binding constants at 150 mM NaCl for the FcR-γ and FcRII dpITAM peptides were determined using a competitor perturbation method as described in Results.

value of −3.1 measured using NaCl. Hence, for all dpITAM peptides investigated here, the ability of salt to disrupt binding is anion-dependent.

Because of the role of phosphorylation on ITAM tyrosines in regulating the affinity of SH2 domain interactions, the pY-binding pockets are expected to have a particularly strong avidity for phosphate. In fact, a phosphate ion was seen in the crystal structure of unligated Src SH2 domain that was crystallized in phosphate buffer (*5*). The ability of phosphate anions to interfere with CD3-ϵ dpITAM peptide binding was examined by adding buffered sodium phosphate to the binding reactions at concentrations ranging from 0 to 250 mM, with a residual NaCl concentration of 150 mM. These results are plotted in Figure 3B. Phosphate had a stronger effect on binding than either F^- or Cl^-. Although the trend is clearly nonlinear, the average value of SK'_{obs} (here defined as the slope of a log−log plot of K_{obs} versus ([NaCl] + [Na_2HPO_4] + [NaH_2PO_4])) was determined to be −4.5. When the data were plotted with respect to total ionic strength (i.e., total sodium concentration), the slope was −3.4. Hence, phosphate is by far the most effective anion at disrupting binding.

The pY-Binding Pocket and the Salt Effect. The influence of the pY-binding pockets on the salt effect was examined in two ways: (i) by determining the effects of removal of either phosphate from the dpITAM peptide and (ii) by examining the salt dependence of the binding of the single amino acid phosphotyrosine.

We first examined the salt dependence of binding of two monophosphorylated ITAM (mpITAM) peptides derived from the FcR-γ ITAM sequence: these are designated NC* and N*C in Table 1, where the asterisk indicates phosphorylation of the C-terminal or N-terminal tyrosine in the ITAM, respectively. Titrations at 150 mM salt are presented in Figure 2B. At this salt concentration, both mpITAM peptides have dramatically reduced affinity as compared to the corresponding dpITAM peptide, and the NC* peptide has higher affinity than the N*C peptide (Table 2): the K_d at 150 mM NaCl increases from ∼2 nM for the FcR-γ dpITAM peptide to 1.31 μM and 7.24 μM for the NC* and N*C mpITAM peptides, respectively. Hence, each phosphate group in the dpITAM peptide makes a sizable contribution to the total free energy of dpITAM peptide binding (3.9 ± 0.3 kcal/mol for the N-terminal phosphate and 4.8 ± 0.2 kcal/mol for the C-terminal phosphate). These values are somewhat smaller than that obtained for the contribution of phosphate in Src SH2 domain−phosphopeptide interactions (5.6 kcal/mol at 100 mM NaCl) (*7*).

The NaCl dependence of binding for the mpITAM peptides is shown in Figure 4A. Binding of both mpITAM peptides was characterized by a markedly lower value of SK_{obs} as compared to dpITAM peptide binding: −1.8 ± 0.2 for the NC* peptide and −1.2 ± 0.2 for the N*C peptide (versus −3.1 for the FcR-γ dpITAM peptide). Thus, the individual phosphate−pY-binding pocket interactions are large contributors to the total salt effect observed for dpITAM peptide binding. As for the dpITAM peptides, the magnitude of the salt dependence of mpITAM peptide binding was considerably reduced when chloride was replaced by fluoride as shown in Figure 4B (see also SK'_{obs} values listed in Table 2).

To assess the degree to which the overall salt dependence of binding is influenced by pY−pY-binding pocket interactions alone, the ability of Ac-pY-NH_2 to perturb binding of the CD3-ϵ dpITAM peptide at various [NaCl] was measured.

The competitive effect of Ac-pY-NH_2 on K_{obs} for the CD3-ϵ dpITAM peptide at 150 mM NaCl was first examined and is shown in Figure 5. According to Wyman linkage theory (*25*), the slope of a plot of log K_{obs} versus log [pY] yields the change in the number of phosphotyrosine molecules bound to the protein upon dpITAM peptide binding:

$$\Delta\langle \mathrm{pY}\rangle = \frac{d \log K_{obs}}{d \log[\mathrm{pY}]} \qquad (1)$$

where a negative slope indicates release of pY. The slope of the fitted line in Figure 5 ranges from −0.6 to −1.9, consistent with the hypothesis that Ac-pY-NH_2 is interacting with Syk-tSH2 at no more than two discrete sites as would

Table 2: Dependence of the Binding Constants on Salt Concentration: Values of SK_{obs} and SK'_{obs} for the Various Tyrosyl Phosphopeptides and Ac-pY-NH_2 Are Reported, as Well as the Values of the Binding Constants at 150 mM NaCl

peptide	salt	range of [salt] (mM)	K_d at 150 mM [NaCl] (nM)	SK_{obs}	SK'_{obs}
			Syk-tSH2 domain		
CD3-ϵ	NaCl	150−1000	20.2 ± 3.5	-2.61 ± 0.05	n/a
FcR-γ	NaCl	150−1000	1.75 ± 0.8	-3.06 ± 0.17	n/a
FcR−II	NaCl	150−1000	1.62 ± 0.8	-2.98 ± 0.26	n/a
NC*	NaCl	150−1000	1300 ± 120	-1.75 ± 0.18	n/a
N*C	NaCl	150−750	7240 ± 1900	-1.16 ± 0.17	n/a
pY[b]	NaCl	150−750	$(7.2 \pm 1) \times 10^6$	-1.19 ± 0.09	n/a
CD3-ϵ	NaF	150−750[a]	n/a		-1.00 ± 0.07
FcR-γ	NaF	150−750[a]	n/a		-1.6[d]
NC*	NaF	150−750[a]	n/a		-0.24 ± 0.05
N*C	NaF	150−750[a]	n/a		-0.22 ± 0.21
pY[c]	NaF	150−750[a]	n/a		-0.65 ± 0.06
			Src SH2 domain		
pYEEI	NaCl	150−1000	340 ± 140	-2.40 ± 0.13	n/a
pYAAI	NaCl	150−575	4540 ± 400	-1.27 ± 0.07	n/a

[a] Total salt concentration includes 150 mM NaCl. [b] Results from fit to eqs 3−5 using data from Figure 6A; K_d at 150 mM NaCl is $1/K_{comp}$, and SK_{obs} corresponds to SK_{comp}. [c] Same as footnote *b*, except using data from Figure 6B. SK'_{obs} corresponds to SK'_{comp}. [d] Derived from only three points (Figure 4B); as explained in the text, the complete range of [NaF] could not be investigated. Uncertainty is not reported because of the limited number of data points.

be expected if it is acting as a competitive inhibitor to binding.

The salt dependence of CD3-ϵ dpITAM peptide binding was next examined at selected Ac-pY-NH_2 concentrations (4, 9, and 15 mM; Figure 6A). As evident in Figure 6A, increasing pY concentrations greatly affects the [NaCl] dependence of dpITAM binding. For example, while in the absence of pY, a 10-fold increase in [NaCl] results in a 400-fold decrease in binding affinity, in the presence of 15 mM pY, a similar increase in [NaCl] results in a 30-fold decrease in affinity. Thus, [pY] appears to greatly modulate the magnitude of the salt effect on binding of dpITAM peptides to the Syk-tSH2 domain, suggesting that a large part of the salt effect is caused by perturbations of electrostatic interactions at the pY-binding pocket.

A more quantitative estimate of the effect of pY on the salt dependence of dpITAM binding was then sought by attempting to extract from the data an apparent value for the salt dependence (defined as SK_{comp}) of Ac-pY-NH_2 binding. As shown in eq 2, measurement of the dependence of the dpITAM binding constant (K_{obs}) on both salt ([S]) and pY concentrations is sufficient to measure SK_{comp}. The

$$SK_{comp} = \frac{\partial \log \Delta\langle pY\rangle}{\partial \log[S]} = \frac{\partial^2 \log K_{obs}}{\partial \log[NaCl]\partial \log[pY]} \quad (2)$$

dependence of K_{obs} on salt concentration is described by eq 3 and that of K_{obs} on [pY] at a given salt concentration is described by eq 4. In eq 3, K^0_{obs} is the dpITAM peptide

$$\log K^0_{obs([S])} = \log K^{0,ref}_{obs} + SK_{obs} \log([S]/[S]_{ref}) \quad (3)$$

$$K_{obs([pY],[S])} = \frac{K^0_{obs([S])}}{(1 + K_{comp([S])}[pY])^2} \quad (4)$$

binding constant in the absence of pY and $K^{0,ref}_{obs}$ is K^0_{obs} at the reference salt concentration ($[S]_{ref}$, 150 mM [NaCl]). To derive eq 4, Ac-pY-NH_2 was assumed to bind to two independent and identical sites with binding constant K_{comp}. Although this may not be mechanistically correct, it accurately describes the log K_{obs} for CD3-ϵ dpITAM peptide binding versus log[pY] binding curve (see Figure 5) and thus will provide an accurate estimate of the dependence of K_{obs} on [pY]. Finally, the salt dependence of K_{comp} is expressed as

$$\log K_{comp_{([S])}} = \log K^{ref}_{comp} + SK_{comp} \log([S]/[S]_{ref}) \quad (5)$$

where K^{ref}_{comp} is the competitor binding constant at the reference salt concentration.

Fitting of the K_{obs} versus [S] and [pY] data in Figure 6A to eqs 3−5 yielded a value for the parameters SK_{comp}, SK_{obs}, $K^{0,ref}_{obs}$, and K^{ref}_{comp}. Fitted curves are shown in Figure 6A, and the parameters SK_{comp} and K^{ref}_{comp} are listed in Table 2. The fitted values for SK_{obs} and $K^{0,ref}_{obs}$ are not reported since they were within error of those measured independently (Figure 3).

A value of -1.2 ± 0.1 for SK_{comp} was obtained. Since there is two pY-binding pockets in the Syk-tSH2 domain, then one can infer an approximate value for the total salt dependence of Ac-pY-NH_2 binding to the Syk-tSH2 domain of ~ -2.4. This compares with the value of SK_{obs} of -2.6 for the CD3-ϵ dpITAM peptide binding, indicating that a large part of the salt dependence of dpITAM binding is caused by disruption of electrostatic interactions at the pY-binding pockets.

The degree to which the pY-binding pockets contribute to the anion selectivity was next examined by repeating the above experiments in NaF. Experiments were conducted and data were analyzed in the same manner as for the pY competition experiments in NaCl, with the exception that the solution contained 150 mM NaCl and a variable concentration of NaF. These results are shown in Figure 6B. Fitting to eqs 3−5 yielded a value of SK'_{comp} of -0.6 ± 0.1 (Table 2). Thus, when only the phosphotyrosine-binding pocket is probed, there is also a large degree of anion selectivity.

Role of Ionic Interactions Outside the pY-Binding Pocket. The fact that there are statistically significant differences in the values of SK_{obs} for different dpITAM sequences suggests

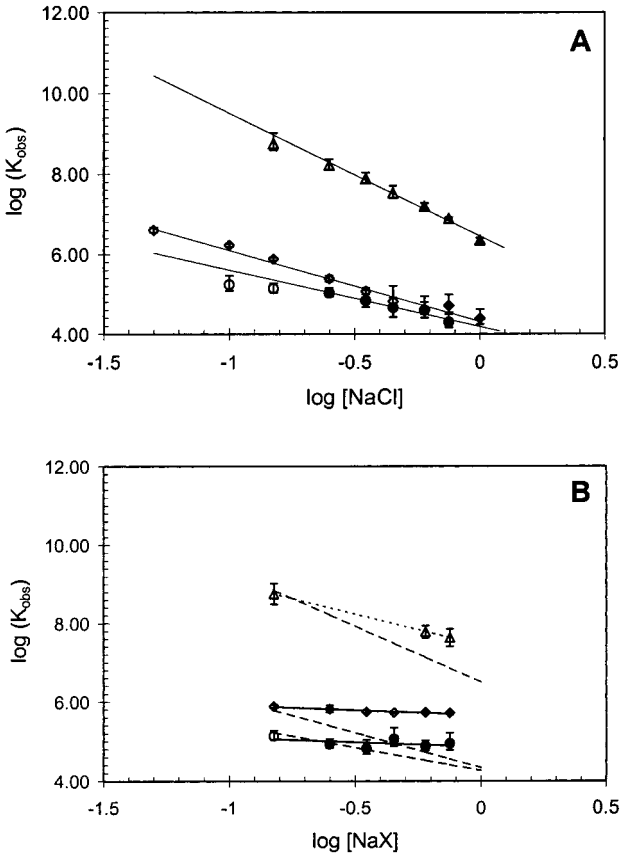

FIGURE 4: Salt dependence of the binding of mpITAM peptides derived from the FcR-γ ITAM sequence. Results for N*C (circle) and NC* (diamond) mpITAM peptide binding are reported (see Table 1 for naming conventions). The dually phosphorylated FcR-γ dpITAM peptide is also shown for comparison (open triangle). Logarithm of binding constants, K_{obs}: (A) as a function of log-[NaCl] (B) as a function of log([NaF] + [NaCl]), where NaCl concentration is constant (150 mM). Linear fits are indicated by solid lines except for the FcR-γ dpITAM peptide in NaF, for which only three points were available (see text); linear fit to these three points is indicated by short dashes. Normal dashes in panel B indicate fitted lines from the NaCl data for mpITAM peptide binding reported in panel A and are shown to facilitate comparison with the NaF data. Filled symbols indicate that the binding constant was determined by a competitive binding assay in which the ligand was used as a competitor against a tighter binding ligand (see Materials and Methods). Linear fits for both panel A and panel B are least-squares fits to the data between 150 and 1000 mM salt concentrations i.e., data below 150 mM salt were not included in the fits.

a role for electrostatic interactions involving residues outside the pY-binding pocket (Figure 3A and Table 2). However, a detailed study of the sequence dependence of SK_{obs} using the Syk-tSH2−dpITAM peptide interaction as a model would be expensive due to the high cost of synthesizing doubly phosphorylated peptide sequences. In contrast, the single SH2 domain of the Src kinase (Src SH2 domain) is more amenable to this kind of investigation. It is also an appropriate system to investigate the role of electrostatic interactions in regions of the binding interface outside the pY-binding pocket. Indeed, binding studies utilizing randomized peptide libraries have shown that the Src SH2 domain has a selection preference for glutamate residues at the +1 and +2 positions C-terminal to the pY (*26*), and these residues have been shown to contribute to binding of the Src SH2 domain to its high affinity consensus pYEEI sequence (*6*). This system was therefore selected for further study.

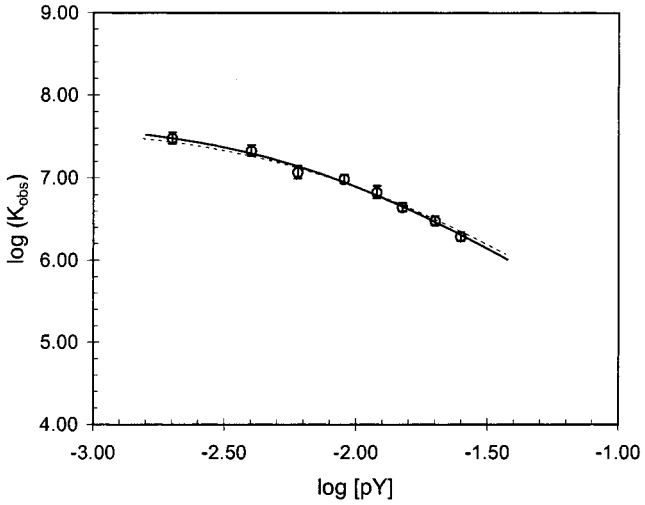

FIGURE 5: Dependence of the binding constant, K_{obs}, for the CD3-ϵ dpITAM peptide on Ac-pY-NH2 concentration. Solid line represents a cubic spline to the data that was used to take the derivative of the plot to determine $\Delta\langle pY\rangle$ (defined in text) in a model-independent manner. Dashed line indicates fit to two independent and identical site model as described by eq 4 and discussed in the text, with parameters shown in Table 2.

Isothermal calorimetry titrations were conducted to study the salt dependence of the interaction of the Src SH2 domain with a peptide containing the high affinity binding consensus sequence pYEEI (referred to hereafter as the pYEEI peptide; see sequence in Table 1). Likewise, the binding of a variant peptide with the two glutamate residues at the +1 and +2 positions C-terminal to the pY mutated to alanine (the pYAAI peptide; Table 1) was characterized. These results are shown in Figure 7. The pYEEI peptide binds tighter than the pYAAI peptide to the Src SH2 domain with a K_d of 0.34 ± 0.14 μM at 150 mM NaCl as compared with 4.54 ± 0.4 μM at 150 mM for the pYAAI peptide, a difference in binding free energy of 1.5 kcal/mol. The salt dependences of these two peptides are also significantly different: the SK_{obs} value for the Src SH2 domain−pYEEI peptide interaction is −2.4 ± 0.1 as compared with a value of SK_{obs} of −1.3 ± 0.1 for the Src SH2 domain−pYAAI peptide interaction (Table 2). Hence, interactions of the +1 and +2 Glu in the peptide with the Src SH2 domain contribute significantly to the total salt effect. These results suggest a role for electrostatic interactions in determining peptide-binding specificity.

Calorimetric titration also enables the direct determination of enthalpies of binding, ΔH°_{obs}. The enthalpies of binding were virtually independent of salt concentration; no detectable trend was observed within confidence limits (65%) for the Src SH2 domain−pYEEI peptide interaction, and there was a modest trend toward more exothermic binding at a higher salt concentration for the Src SH2 domain−pYAAI peptide interaction, with a decrease in ΔH°_{obs} of 0.3 ± 0.1 kcal/mol per order of magnitude salt concentration change (data not shown). Experiments conducted under slightly different solution conditions[3] measuring the salt dependence of Syk-tSH2−dpITAM peptide interactions at various temperatures showed no detectable trend in the value of SK_{obs}

[3] Glycine (150 mM) was included as an additive for high-temperature stabilization. Otherwise, conditions were the same as those outlined in Materials and Methods.

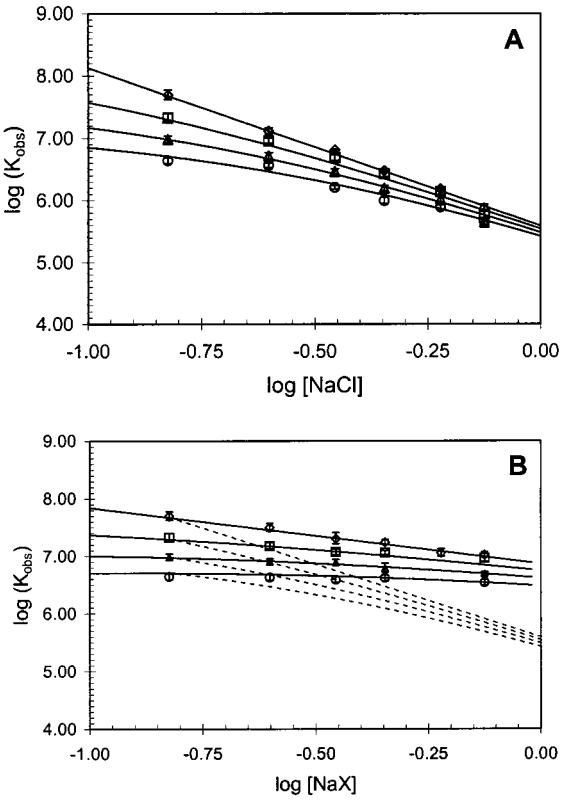

FIGURE 6: NaCl (A) and NaF (B) dependence of the binding constant for the CD3-ϵ dpITAM peptide at varying concentrations of Ac-pY-NH2. The logarithm of the binding constant, log(K_{obs}), is plotted as a function of (A) log([NaCl]) (B) log([NaF] + [NaCl]), where [NaCl] is constant (150 mM). Ac-pY-NH2 concentrations are 0 (open diamond), 4 (open square), 9 (open triangle), and 15 (open circle) mM. Solid lines in panels A and B represent a fit to eqs 3−5. In panel B, the dashed lines represent the fits to the NaCl data reported in panel A and are shown to facilitate comparison with the NaF data. Error bars represent 95% confidence intervals. For the NaCl data, seven additional points at various concentrations of Ac-pY-NH2, including the points reported in Figure 5, were incorporated into the analysis but are omitted here for clarity.

between 7.5 and 30 °C (unpublished data). Therefore, by van't Hoff analysis, we can conclude that the enthalpy associated with the interaction of NaCl with the binding partners is very close to zero for Syk-tSH2−dpITAM peptide interactions, as it is for the interactions between the Src SH2 domain and the ligands studied here.

DISCUSSION

In the study presented here, we have probed the role of electrostatics in tyrosyl phosphopeptide−SH2 domain interaction by investigating the salt dependence of binding of two SH2 domain systems, the single SH2 domain of the Src kinase and the tandem SH2 domain of the Syk kinase. We show here that salt strongly effects the binding energetics of tyrosyl phosphopeptide recognition by these SH2 domains and that a large part of this effect is due to anion-dependent perturbation of electrostatic interactions at the pY-binding pocket.

Magnitude of the Salt Effect. The free energies of binding of dually and singly tyrosine-phosphorylated peptides to the Syk-tSH2 and the Src SH2 domains are significantly dependent on salt (Figures 3A and 7). A change of 1 order of magnitude in NaCl concentration can reduce the magnitude

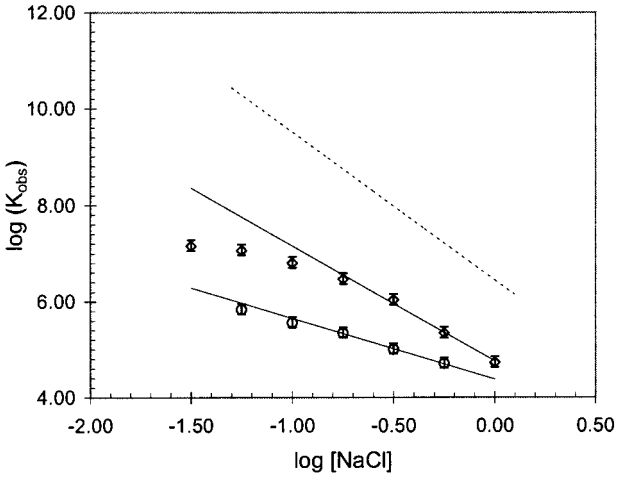

FIGURE 7: NaCl dependence of the binding contants for the Src SH2 domain interactions with the pYEEI (open diamond) and pYAAI (open circle) peptides determined by isothermal titration calorimetry. Each point represents the average of 2−3 experiments. Solid lines represent linear regression to data at 178 mM NaCl and above. The dashed line is the regression from the salt dependence of CD3-ϵ dpITAM peptide binding to Syk-tSH2 shown for comparison.

of the binding free energy by >3 kcal/mol; the effect is even more pronounced when sodium phosphate is used to perturb binding (Figure 3B).

Protein−protein and protein−peptide interactions are not necessarily strongly dependent on salt concentration. Several protein−protein interactions have been shown to exhibit little or no salt dependence [for examples, see the self-association of the N-terminal domain of the λcI repressor or the binding of histidine-containing phospho carrier protein (Hpr) to HPr-specific monoclonal antibodies (*27, 31*)]. The binding of a peptide derived from the 0.5 β HIV-1 antibody (a neutralizing antibody to HIV1) to the RP135 peptide (a fragment of the V3 loop of the capsid gp120 protein), where at least two salt bridges are known to make important contributions, was weakened by only 1.6 kcal/mol when the salt concentration was changed from 0 to 1 M (*28*). However, some protein−protein interactions exhibit greater salt dependence. For example, thrombin binding to the highly charged 10 residue C-terminal tail of the inhibitor hirudin (which forms three salt bridges at the interface) is characterized by SK_{obs} of −1.1, whereas binding of the entire 65-residue hirudin peptide, which contains three additional salt bridges is characterized by SK_{obs} of −1.2, only slightly higher in magnitude than that for the C-terminal tail. Thrombin binding to the cofactor thrombomodulin is characterized by a SK_{obs} of −2.3 in the absence of a chondroitin sulfate moiety attached to the cofactor, whereas the magnitude increases to −5.4 in the presence of the chondroitin sulfate moiety, which is believed to interact with the protein. Altogether, these findings are consistent with what is observed here for the SH2 domain−phosphopeptide interactions: polypeptide electrostatic interactions are characterized by a modest but significant salt dependence, while much larger contributions to the salt dependence are made by specific interactions involving doubly charged ionic groups such as phosphate or sulfate.

Differential Anion Effects and Localization of the Salt Effect to the pY-Binding Pocket. The type of salt used to probe binding dramatically influences the sensitivity of the

free energy of the SH2 domain−phosphopeptide interaction to salt concentration. The two sodium halides NaCl and NaF have markedly different effects: Cl^- perturbs binding much more efficiently than F^-. The weaker effect of NaF could be due at least in part to the water-ordering property of this salt. However, this effect is expected to be negligible at low NaF concentrations; yet the reduced effect of NaF as compared to NaCl on binding is apparent even at the lowest concentrations of salt. Phosphate ions also have a significant effect on binding of tyrosyl phosphopeptides. For example, 50 mM sodium phosphate is able to reduce the affinity of the CD3-ϵ dpITAM peptide for Syk-tSH2 by a factor of 10, even when competing with 150 mM NaCl (Figure 3B).

One region of the binding interface that is especially likely to affect the salt dependence of binding is the pY-binding pocket. Indeed, clear electron density for a phosphate ion was observed in this region of the structure of the Src SH2 domain crystallized in the presence of 200 mM sodium phosphate (*5*). This hypothesis was tested by examining the salt dependence of binding of mpITAM peptides and of pY alone. Marked reductions in the magnitude of $S K_{obs}$ were observed for mpITAM peptide binding as compared to dpITAM peptide binding (Figure 4A; Table 2). Moreover, NaF was found to be ineffective at perturbing binding of mpITAM peptides (Figure 4B; Table 2). These results are consistent with the interpretation that a large part of the salt effect in NaCl is attributable to the perturbation of electrostatic interactions at the pY-binding pockets.

Examination of the salt dependence of binding of phosphotyrosine alone leads to similar conclusions. Binding of one molecule of the single amino acid Ac-pY-NH_2 is also strongly dependent on salt (approximated by the value of $S K_{comp} = -1.2$). Since there are two pY-binding pockets in the Syk-tSH2 domain, then binding of two phosphotyrosines would result in a log−log salt dependence of -2.4 ± 0.3, which is nearly as large as that observed upon binding of the 19-residue CD3-ϵ dpITAM peptide to the same SH2 domain (-2.6 ± 0.1). Moreover, as with dpITAM peptide binding, NaF is not as effective as NaCl in perturbing binding of pY alone. Altogether, these findings clearly ascribe a large part of the salt effect to the pY-binding pockets and are consistent with the interpretation that electrostatic interactions predominate in these regions of the Syk-tSH2 domain−tyrosyl phosphopeptide interface.

SK_{obs} and Peptide Binding Specificity of SH2 Domains. Because of the ability of salt to screen electrostatic interactions, the magnitude of the salt effect is expected to be correlated with the degree of favorable electrostatic interactions at the binding interface. Here we show that, for the Syk-tSH2 and Src SH2 domain systems, values of $S K_{obs}$ are in general more negative for binding of higher affinity peptides, suggesting that the screening of electrostatic interactions involving residues other than pY significantly contributes to the salt effect. This is especially clear from the results obtained on the Src SH2 domain and its interaction with the high affinity pYEEI peptide and a site specific variant of that ligand, which show that interactions involving the glutamate side chains at the +1 and +2 positions of the ligand make significant contributions to the salt dependence of binding (Figure 7 and Table 2). In fact, the interaction between the pYEEI peptide and the Src SH2 domain exhibits nearly as high of a NaCl dependence as that for the Syk-tSH2−dpITAM peptide interaction. Clearly, then, charged residues other than pY can contribute significantly to the overall salt dependence. These results point to a possible role of electrostatic interactions in peptide binding specificity and suggest that higher affinity in an optimal SH2 domain−tyrosyl phosphopeptide interaction may partially result from electrostatic complementarity between surfaces in the SH2 domain and in the peptide.

CONCLUSIONS

A goal of molecular recognition studies is the prediction of energetic properties of a macromolecular interaction from structure. A necessary step in this process is the identification of quantifiable structural properties that are correlated with experimentally accessible thermodynamic variables. Before this is accomplished, it is necessary to thoroughly characterize the reaction being observed by identifying linked processes that might complicate the interpretation of the variable under investigation. Identification of these linked processes leads to a more thorough understanding of the energetic states accessible to the macromolecule in question that are often of biological importance.

In this work, examination of the dependence of the free energy of binding on salt concentration demonstrated the linkage between tyrosyl phosphopeptide binding and ion effects localized to the pY-binding pockets of SH2 domains. This finding suggests a role for phosphate and chloride as modulators of tyrosyl phosphopeptide binding in vivo. Indeed, as suggested by the continuum electrostatic potential calculations presented in Figure 1D, binding of phosphate, for example, would substantially alter the electrostatic potential distribution at the phosphotyrosine binding site. Chloride is present in the cytosol, as is phosphate. Moreover, because of the membrane potential, an anion gradient is likely to form near the membrane, with the low concentration end of this gradient closer to the membrane (*29*). Hence, proximity of SH2 domain-containing proteins to the membrane during signaling may result in increased affinity for their tyrosine-phosphorylated docking sites on activated receptors.

Another significant finding in the study presented here is that higher affinity binding may correlate with a greater dependence on salt concentration. Electrostatic interactions are likely to be involved in determining peptide binding specificity, at least in the two SH2 domain systems investigated here. These observations suggest that high affinity binding may arise from the ability of the peptide ligand to electrostatically complement the interacting surfaces of the SH2 domains.

ACKNOWLEDGMENT

We thank Drs. T. M. Lohman and J. I. Gordon for use of equipement and Drs. T. M. Lohman, A. B. Herr, A. G. Kozlov, and E. Di Cera for comments.

REFERENCES

1. Sadowski, I., Stone, J. C., and Pawson, T. (1986) *Mol. Cell. Biol. 6*, 4396−4408.
2. Pawson, T., and Scott, J. D. (1997) *Science 278*, 2075−2080.
3. Kuriyan, J., and Cowburn, D. (1997) *Annu. Rev. Biophys. Biomol. Struct. 26*, 259−288.

4. Waksman, G., Kominos, D., Robertson, S. R., Pant, N., Baltimore, D., Birge, R. B., Cowburn, D., Hanafusa, H., Mayer, B. J., Overduin, M., Resh, M. D., Rios, C. B., Silverman, L., and Kuriyan, J. (1992) *Nature 358*, 646−653.
5. Waksman, G., Shoelson, S. E., Pant, N., Cowburn, D., and Kuriyan, J. (1993) *Cell 72*, 779−790.
6. Bradshaw, J. M., and Waksman, G. (1999) *Biochemistry 38*, 5147−5154.
7. Bradshaw, J. M., Mitaxov, V., and Waksman, G. (1999) *J. Mol. Biol. 293*, 971−985.
8. Bradshaw, J. M., Mitaxov, V. M., and Waksman, G. (2000) *J. Mol. Biol. 299*, 549−563.
9. Bradshaw, J. M., and Waksman, G. (1998) *Biochemistry 37*, 15400−15407.
10. Reth, M. (1989) *Nature 338*, 383−385.
11. Cambier, J. C. (1995) *J. Immunol. 152*, 3281−3285.
12. Stone, S. R., Dennis, S., and Hofsteenge, J. (1989) *Biochemistry 28*, 6857−6863.
13. De Cristofaro, R., Fenton, J. W. D., and Di Cera, E. (1992) *J. Mol. Biol. 226*, 263−269.
14. Record, M. T., Jr., Zhang, W., and Anderson, C. F. (1998) *Adv. Protein Chem. 51*, 281−353.
15. Lohman, T. M., Overman, L. B., Ferrari, M. E., and Kozlov, A. G. (1996) *Biochemistry 35*, 5272−5279.
16. Kenar, K. T., Garcia-Moreno, B., and Freire, E. (1995) *Protein Sci. 4*, 1934−1938.
17. Ayala, Y., and Di Cera, E. (1994) *J. Mol. Biol. 235*, 733−746.
18. Fütterer, K., Wong, J., Grucza, R. A., Chan, A. C., and Waksman, G. (1998) *J. Mol. Biol. 281*, 523−537.
19. Grucza, R. A., Futterer, K., Chan, A. C., and Waksman, G. (1999) *Biochemistry 38*, 5024−5033.
20. Bradshaw, J. M., Grucza, R. A., Ladbury, J. E., and Waksman, G. (1998) *Biochemistry 37*, 9083−9090.
21. Cousins-Wasti, R. C., Ingraham, R. H., Morelock, M. M., and Grygon, C. A. (1996) *Biochemistry 35*, 16746−16752.
22. Gill, S. C., and von Hippel, P. H. (1989) *Anal. Biochem. 182*, 319−326.
23. Collins, K. D. (1995) *Proc. Natl. Acad. Sci. U.S.A. 92*, 5553−5557.
24. Nightingale, E. R., Jr. (1959) *J. Phys. Chem. 63*, 1381−1387.
25. Wyman, J., Jr. (1964) *Adv. Protein Chem. 19*, 223−286.
26. Songyang, Z., Shoelson, S. E., Chaudhuri, M., Gish, G., Pawson, T., Haser, W. G., King, F., Roberts, T., Ratnofsky, S., Lechleider, R. J., et al. (1993) *Cell 72*, 767−778.
27. Smallshaw, J. E., Brokx, S., Lee, J. S., and Waygood, E. B. (1998) *J. Mol. Biol. 280*, 765−774.
28. Faiman, G. A., Levy, R., Anglister, J., and Horovitz, A. (1996) *J. Biol. Chem. 271*, 13829−13833.
29. Rostovtseva, T. K., Aguilella, V. M., Vodyanoy, I., Bezrukov, S. M., and Parsegian, V. A. (1998) *Biophys. J. 75*, 1783−1792.
30. Honig, B., Sharp, K., and Yang, A.-S. (1993) *J. Phys. Chem. 97*, 1101−1109.
31. Bain, D. L., and Ackers, G. K. (1994) *Biochemistry 33*, 14679−14689.

BI000891N